Detecting Rain With QuikScat

Carl A. Mears, Deborah Smith, and Frank J. Wentz
Remote Sensing Systems, 438 First Street, Suite 200, Santa Rosa, CA 95401
(707) 545-2904 ext. 21(Voice)/(707) 545-2906 (FAX)/mears@remss.com (email)

ABSTRACT

The wind retrievals produced from the QuikScat Scatterometer[1] are affected by the presence of rain. Scattering from the rain drops and from surface roughness caused by rain-induced splashing increases the measured signal power. The rain also attenuates the signal as it travels to and from the sea surface, reducing its power. At low wind speeds, the scattering effects dominate, causing the inferred wind-induced radar cross-section and therefore the wind speed to be over estimated. At high winds, attenuation becomes more important. In order to detect rain-contaminated winds, we have developed a rain-detection algorithm based on how well the measured radar cross-sections fit the NSCAT-2 model function[2] that was used to retrieve the winds. We report an analysis of the performance of our algorithm. At low wind speeds, our algorithm may be a more sensitive measure of rain than microwave-radiometer-based methods. We also report the results of a study where we attempt to use QuikScat measurements, in conjunction with winds modeled by a general circulation model, to deduce rain rates over the world's oceans.

RAIN AND SCATTEROMETER MEASUREMENTS

Scatterometers such as QuikScat obtain the surface wind vector over the ocean by measuring the radar signal returned from the sea surface. The sea surface radar cross section, σ_0, is measured for several different azimuth angles and for both horizontally and vertically polarized radiation. The wind vector can be retrieved by fitting these measurements to a geophysical model function that describes the expected σ_0 as a function of wind speed, wind direction relative to the instrument look angle, and the incidence angle. The presence of rain in the atmosphere through which the radar signal is traveling affects the measured σ_0. This occurs in three ways.

- The radar signal is attenuated by the rain as it travels to and from the earth's surface. This reduces the measured σ_0.
- The radar signal is scattered by the rain drops. Some of this scattered power returns to the instrument. This increases the measured σ_0.
- The roughness of the sea surface is increased because of splashing due to rain drops. This increases the measured σ_0.

A simple expression for the measured cross-section σ_{meas} that describes the measured σ_0 with these effects included is shown below.

$$\sigma_{meas} = \sigma_{scat}(R) + \tau(R)^2\left[\sigma_{wind} + \sigma_{splash}(R/h)\right]. \quad (1)$$

In this equation, R is the columnar rain rate (rain rate times column height h), σ_{scat} is the contribution due to scattering from rain drops, τ is the one-way attenuation due to the rain, σ_{wind} is the contribution due to surface roughness caused by wind, and σ_{splash} is the contribution due to surface roughness caused by raindrops. At low wind speeds, where σ_{wind} is small, the additional scattering effects (σ_{scat} and σ_{splash}) dominate, and σ_{meas} is greater than σ_{wind}. Eventually, as the wind speed increases, σ_{wind} becomes large enough that the attenuation effect becomes important, and begins to cancel the effect of the scattering terms.

THE EFFECT OF RAIN ON QUIKSCAT

For the angles of incidence and the radar frequency used by QuikScat, the scattering effect is dominant up to a wind speed of about 10 m/s, and the scattering and attenuation effects cancel completely at a wind speed between 15 m/s and 20 m/s, depending on the relative wind direction and which beam (h-pol or v-pol) is being considered. At low wind speeds, it is fairly easy to detect when a QuikScat measurement is affected by rain. For low winds, the h-pol σ_{wind}, $\sigma_{H,wind}$ is significantly (~3 dB) smaller than the v-pol σ_{wind}, $\sigma_{V,wind}$. The rain-scattered contribution is either polarization independent (for small, spherical rain drops) or has a larger h-pol component (for large, flattened rain drops)[3]. When the rain-scattered component is added into the sea-surface component, σ_H is too large compared to σ_V to be consistent with any wind speed and direction. For higher wind speeds or very high rain rates, the situation is not so favorable. As the wind speed increases, $\sigma_{H,wind}$ increases faster than $\sigma_{V,wind}$. For some wind directions at high wind speed $\sigma_{H,wind}$ exceeds $\sigma_{V,wind}$. The magnitudes of σ_{wind} for both polarizations is also much larger, and the scattering component of σ_{meas} becomes less important. Under these conditions, the presence of rain modifies σ_H and σ_V, but usually not by so much that they become inconsistent with any wind vector. Instead, the wind vectors are typically changed in magnitude and rotated to be aligned slightly more perpendicular to the track of the satellite. The $\sigma_{H,wind}$ to $\sigma_{V,wind}$ ratio in the model function is maximized when the retrieved vector is aligned perpendicular to the satellite track.

Rain is more highly variable over short distances than is the wind. For each 25 km wind vector cell, typically ~12 separate σ_0 measurements are used to retrieve the wind vector. These individual measurements, which may be separated by more the 25 km, may view significantly different rain rates. Observations of the sea surface from the same direction and with the same polarization, and therefore would usually measure similar values of σ_0, might show significant variation. This, too, can form a component of a rain detection algorithm.

A RAIN DETECTION ALGORITHM

We have developed a rain detection algorithm that is simple, and sensitive to both the σ_H to σ_V ratio, and to high variability within a wind vector cell. The algorithm is based on an empirically normalized objective function (ENOF), which is defined for each wind vector cell.

$$ENOF = \frac{1}{N}\sum_{i=1}^{N}\frac{\left(\sigma_{i,MEAS} - \sigma_{i,NSCAT2}\right)^2}{W_i} \quad (2)$$

0-7803-6359-0/00/$10.00 © 2000 IEEE

Here, $\sigma_{i,MEAS}$ is the measured σ_0 for each observation in the cell, and $\sigma_{i,NSCAT\text{-}2}$ is the value of σ_0 calculated for each observation, using the retrieved wind vector and the NSCAT-2 model function used to retrieve the wind. W_i is a weighting function that represents the "expected" or "typical" contribution of the i_{th} measurement to the overall variance, and the sum is over the N observations used to retrieve the wind vector for the cell. W_i is chosen, using the procedure described in the next paragraph, so that if the ENOF is greater than one, the fit of the measured σ_0's to the model function is significantly worse than is typical.

Choosing the weights W_i so that the ENOF will be large in the presence of rain is somewhat complicated. Formally, W_i is a function of the true wind speed, the wind direction relative to the observation azimuth angle, the incidence angle, and the polarization. Due to the two-beam conical scanning geometry of QuikScat, we can replace the dependence on the incidence angle and polarization with a dependence on beam index. Previous work[4] has indicated that the expected variance is not a strong function of relative wind direction. The largest problem occurs because we do not know the true wind speed. Using the retrieved wind speed is not acceptable because the typical effect of rain is to increase all σ_0 measurements, yielding a retrieved wind speed that is much higher than the true wind speed. This in turn would give us a much too large value for W_i, and we would be less sensitive to rain-induced increases in variance. Instead of using the retrieved wind, we use a rain-desensitized proxy for wind speed to describe the wind speed dependence. We have constructed a simple wind-speed retrieval regression based on a rain-desensitized average σ_0 given by

$$\overline{\sigma}_{0,rain-desensitized} = \overline{\sigma}_V - 0.5\overline{\sigma}_H(1.0 - 0.05\overline{\sigma}_H), \quad (3)$$

where σ_V and σ_H are the averaged V-pol and H-pol σ_0's for all observations in the cell. Since the presence of rain often increases σ_H more than σ_V , by subtracting away part of σ_H we can construct an average σ_0 that is less sensitive to increases due to rain. At high winds, and therefore large values of σ_0, the value of σ_H approaches that of σ_V, so we reduce the degree to which σ_H is subtracted. This average σ_0 is then used in a polynomial regression of the following form to retrieve a pseudo wind speed.

$$W_{PSEUDO} = a_{1/2}\sigma_0^{1/2} + a_1\sigma_0 + a_2\sigma_0^2 + a_3\sigma_0^3 + a_4\sigma_0^4. \quad (4)$$

The coefficients $a_{1/2}$ – a_4 are chosen by fitting this wind to that retrieved by the full model function.

We then use this pseudo wind speed to divide the measurements into bins by polarization, cross-swath cell number, and wind speed. We only used QuikScat measurements that were completely surrounded by rain free SSM/I measurements. It is likely that SSM/I cells adjacent to a rainy cell also have some rain that is not detected. By excluding both collocated and neighboring QuikScat cells, we ensure that these observations are not used. We used all rain-free collocated measurements for QuikScat rev numbers 900-999. For each bin, a histogram of squared-difference deviations was calculated, and W_i was set to the value of the 95th percentile. We use the 95th percentile, rather than the mean, to help account for variations in the width of the distribution of squared-difference deviations for different cells, wind speeds, and polarizations.

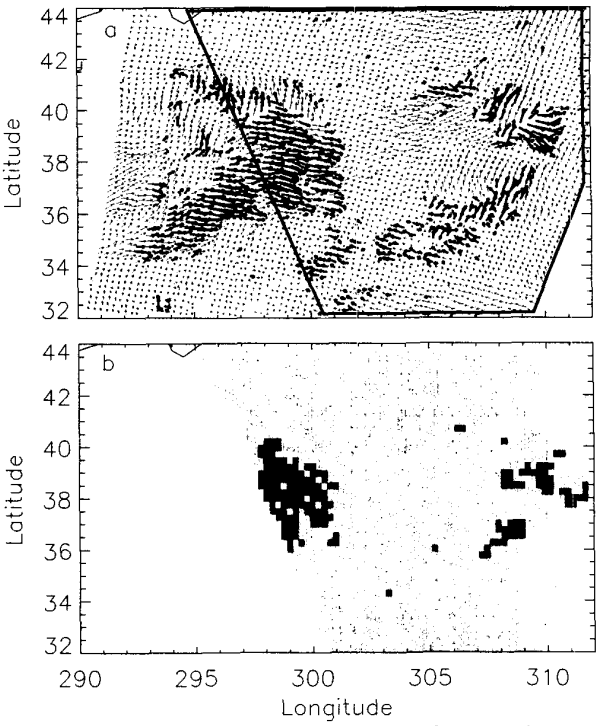

Fig. 1. (a) Wind vectors retrieved using QuikScat for the northwestern Atlantic Ocean on August 26, 1999. The thicker vectors are those flagged as rainy by our algorithm. (b) SSM/I columnar rain rate for the same day, measured within 30 minutes of the QuikScat observation. The light grey are rain free areas, medium grey are rainy areas with a columnar rain rate between 0.1 km×mm/hr and 2.0 km×mm/hr and dark grey denotes rainy areas with rain rates in excess of 2.0 km×mm/hr. White areas represent cells without collocated SSM/I observations. The region of (a) for which SSM/I observations exist is surrounded by the irregular polygon.

Using this empirical weighting, we have an valid expression for the ENOF rain index. The rain detection algorithm is completed by setting a threshold for the ENOF index above which we say that it is raining. By adjusting this threshold, we can adjust the global rate at which cells are flagged as being contaminated by rain. For the results discussed below, the threshold is set so that about 7.5% of the data are flagged as rain contaminated. In Fig. 1, we present an anecdotal comparison between our rain flag and the columnar rain rate measured by SSM/I. In this case, nearly all the cells measured to contain significant rain by SSM/I are also flagged as rainy by our algorithm. We also find additional cells that contain rain that are not measured to be so by SSM/I. The wind vectors in these cases show the typical features of rain contaminated winds -- higher wind than neighboring cells, and the wind direction rotated toward the cross-swath direction, suggesting that these wind vectors were not flagged erroneously, and that our algorithm may be more sensitive to rain than radiometer based methods.

The rain in this example occurred in a region of low wind speed, making the rain easy to detect using our method. In regions of higher wind speed, the agreement with SSM/I rain measurements was significantly reduced. In order to evaluate the performance of the rain flagging method on a global scale, we compared the ENOF rain flag to the SSM/I columnar rain rate over a two week period and accumulated

two statistics. The first is the false alarm rate, which is defined as the fraction of SSM/I rain free observations that we flag as having rain. The second is the missed rain rate, which is the fraction of SSM/I observations that indicate significant rain that we do not flag as having rain. We define significant rain as a columnar rain rate in excess of 2.0 km×mm/hr. We would like both these statistics to be as close to zero as possible, but zero values are unlikely due to the high temporal and spatial variation in rain events. Note that

Table I

Wind Speed	False Alarm Rate	Missed Rain Rate
0 – 7 m/s	5.2 %	19.6 %
7 – 14 m/s	4.7 %	38.7 %
> 14 m/s	4.3 %	81.1 %
All Winds	5.4 %	36.3 %

observations for which SSM/I indicates a low, but nonzero rain rate, between 0.1 and 2.0 km×mm/hr do not contribute to the false alarm rate or the missed rain rate. We report these statistics in Table I for three wind speed bins to show how the performance of the algorithm changes with wind speed. The results were binned using surface winds from the National Center for Environmental Prediction (NCEP) analysis. The excellent low-wind-speed agreement with SSM/I decreases strongly with increasing wind speed, for the reasons described above.

RAIN RATES DERIVED FROM QUIKSCAT

The strong influence of rain on the QuikScat measurements led us to suspect that we could also retrieve rain rates (as opposed to the possible presence of rain) from QuikScat observations. We have developed an rain-rate algorithm that uses QuikScat σ_0 observations and surface winds from the European Centre for Medium-range Weather Forecasting (ECMWF) global analysis. To retrieve rain rates we analyze the difference $\sigma_{H,diff}$ between the measured QuikScat H-Pol σ_0's and those calculated using the NSCAT-2' model function and the modeled surface winds. The difference in σ_H could be due to the presence of rain, differences between the actual surface wind and those modeled by the surface analysis, errors in the model function, or random errors in the σ_H measurement. If we assume that large positive differences are due to the presence of rain, we can assign a rain rate using the following two-threshold linear algorithm.

$\sigma_{H,diff} < \sigma_1$ Rain Rate = 0
$\sigma_1 < \sigma_{H,diff} < \sigma_2$ Rain Rate = $m_1 \times (\sigma_{H,diff} - \sigma_1)$
$\sigma_2 < \sigma_{H,diff}$ Rain Rate = $m_1 \times (\sigma_2 - \sigma_1) + m_2 \times (\sigma_{H,diff} - \sigma_2)$

The thresholds σ_1 and σ_2, and the slopes m_1 and m_2 were chosen so that histograms of the rain rate matched those measured by SSM/I as closely as possible over 3 separate wind speed regimes, 0-7 m/s, 7-14 m/s and >14 m/s. The two separate linear regimes with different slopes were required to simultaneously match the SSM/I rain rate histograms at low and high rain rates. In Fig. 2, we show global maps of a 5 day average of the rain rate derived using this algorithm, and the average rain rate measured by SSM/I. While the two maps are not identical, most of the features in the QuikScat-derived rain map correspond to features in the SSM/I rain map, indicating the our procedure does indicate the presence of rain. The are a few features, such as the region of QuikScat derived rain in the North Atlantic near the top of the map, that may be due to errors in the modeled surface winds. These results demonstrate the possibility of using scatterometer measurements to deduce rain rate over the oceans, given the existence of sufficiently accurate surface winds from an alternate source.

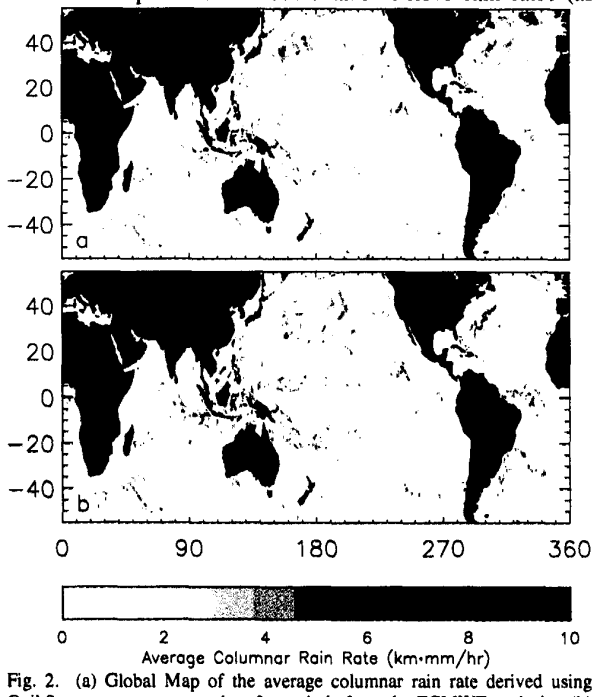

Fig. 2. (a) Global Map of the average columnar rain rate derived using QuikScat measurements and surface winds from the ECMWF analysis. (b) Average columnar rain rate measured using SSM/I. Both maps are five-day averages of collocated observations for February 6-10, 2000

ACKNOWLEDGMENT

This work was supported by NASA JPL Contract Number 960644. We would like to thank ECMWF and NCEP for providing surface analysis data to the QuikScat Cal-Val team

REFERENCES

[1] C. Wu, J. Graf, M. Freilich, D. G. Long, M. Spencer, W. Tsai, D. Lisman, and C. Winn, "The Seawinds Scatterometer Instrument," Proceedings of the International Geoscience and Remote Sensing Symposium, Pasadena, California, 1994.

[2] F. J. Wentz and D. K. Smith, "A model function for the ocean-normalized radar cross section at 14 GHz derived from NSCAT observations," *Journal of Geophysical Research*, vol. 104, pp. 11499-11514, 1999.

[3] T. A Seliga and V. N. Bringi, "Potential use of radar reflectivity measurements at orthogonal polarizations for measuring precipitation," Journal of Applied Meteorology, vol 18, pp. 69-76, 1976.

[4] F. J. Wentz, "Specifying the NSCAT MLE Expected Variance Using the After-the-Fit Sigma0 Residual," RSS Technical Memo Number 121097, Remote Sensing Systems, Santa Rosa 1997.